JOURNAL OF VIROLOGY, Dec. 2011, p. 12201–12215 Vol. 85, No. 23
0022-538X/11/$12.00 doi:10.1128/JVI.06048-11


# A Double-Inactivated Severe Acute Respiratory Syndrome Coronavirus Vaccine Provides Incomplete Protection in Mice and Induces Increased Eosinophilic Proinflammatory Pulmonary Response upon Challenge▽

Meagan Bolles,[1]† Damon Deming,[1]† Kristin Long,[2] Sudhakar Agnihothram,[3] Alan Whitmore,[2] Martin Ferris,[2] William Funkhouser,[4] Lisa Gralinski,[3] Allison Totura,[1] Mark Heise,[1,2,5] and Ralph S. Baric[1,3]*

*Department of Microbiology and Immunology, University of North Carolina at Chapel Hill, Chapel Hill, North Carolina[1]; Carolina Vaccine Institute, University of North Carolina at Chapel Hill, Chapel Hill, North Carolina[2]; Department of Epidemiology, University of North Carolina at Chapel Hill, Chapel Hill, North Carolina[3]; Department of Pathology, University of North Carolina School of Medicine, Chapel Hill, North Carolina[4]; and Department of Genetics, University of North Carolina at Chapel Hill, Chapel Hill, North Carolina[5]*

Received 22 August 2011/Accepted 8 September 2011

**Severe acute respiratory syndrome coronavirus (SARS-CoV) is an important emerging virus that is highly pathogenic in aged populations and is maintained with great diversity in zoonotic reservoirs. While a variety of vaccine platforms have shown efficacy in young-animal models and against homologous viral strains, vaccine efficacy has not been thoroughly evaluated using highly pathogenic variants that replicate the acute end stage lung disease phenotypes seen during the human epidemic. Using an adjuvanted and an unadjuvanted double-inactivated SARS-CoV (DIV) vaccine, we demonstrate an eosinophilic immunopathology in aged mice comparable to that seen in mice immunized with the SARS nucleocapsid protein, and poor protection against a nonlethal heterologous challenge. In young and 1-year-old animals, we demonstrate that adjuvanted DIV vaccine provides protection against lethal disease in young animals following homologous and heterologous challenge, although enhanced immune pathology and eosinophilia are evident following heterologous challenge. In the absence of alum, DIV vaccine performed poorly in young animals challenged with lethal homologous or heterologous strains. In contrast, DIV vaccines (both adjuvanted and unadjuvanted) performed poorly in aged-animal models. Importantly, aged animals displayed increased eosinophilic immune pathology in the lungs and were not protected against significant virus replication. These data raise significant concerns regarding DIV vaccine safety and highlight the need for additional studies of the molecular mechanisms governing DIV-induced eosinophilia and vaccine failure, especially in the more vulnerable aged-animal models of human disease.**

Emerging in 2002 in Guandong Province, China, severe acute respiratory syndrome (SARS) presented as an atypical pneumonia with an overall mortality rate of 10 to 12%, but exceeding 50% in aged (>60-year-old) populations (3, 12, 36). The etiological agent was the novel SARS coronavirus (SARS-CoV), a zoonotic virus that likely emerged from bats and spread into civets and raccoon dogs either concurrent with or prior to the human epidemic (8, 22, 62). While the epidemic strain was controlled by aggressive public health intervention strategies, the possibility of a reemergence is fueled by the presence of SARS-like CoV strains circulating in animal reservoirs (22, 23, 35). Indeed, phylogenetic analysis of outbreak strains isolated during the late 2003/early 2004 epidemic suggest multiple independent emergences into the human population (49, 62).

SARS-CoV is a cytoplasmically replicating, positive-polarity, single-stranded RNA (ssRNA) virus with three major membrane-bound structural proteins, spike (S), envelope (E), and membrane (M); several unique glycoproteins; and one structural protein within the virus core, the nucleocapsid (N) protein. Multiple candidate antiviral and immunomodulatory therapeutics have been developed in response to the epidemic, and vaccines would likely be a major tool in controlling any new SARS-CoV outbreak (51). Key to the development of effective SARS vaccines appears to be the generation of neutralizing antibodies targeting the S glycoprotein, which provide complete protection upon passive transfer and are consistently associated with protection in multiple vaccine formulations (15, 44, 52, 67). SARS vaccine strategies consist of varied formulations of inactivated (24, 40), live attenuated (33), recombinant subunit (41), DNA (28, 60), or subunit-vectored vaccines (2, 11, 13, 48). Live attenuated vaccines with deletions

* Corresponding author. Mailing address: University of North Carolina at Chapel Hill, 3304 Michael Hooker Research Center, CB 7435, Chapel Hill, NC 27599-7435. Phone: (919) 966-3895. Fax: (919) 966-0584. E-mail: rbaric@email.unc.edu.
† These authors contributed equally to this work.
▽ Published ahead of print on 21 September 2011.

in nonessential proteins show some efficacy in young mice, but low antibody titers preclude sterilizing immunity, and they remain untested in more vulnerable aged animals (33). Vectored vaccines incorporating the spike glycoprotein alone show significant protection but are limited by strain specificity and immunosenescence (48). Inactivated whole-virus vaccines have the advantages of relative ease of production in large quantities, stable expression of conformation-dependent antigenic epitopes, and the contribution of multiple viral immunogens. However, the disadvantages of inactivated formulations include the risk of vaccine preparations containing infectious virus, as well as the inclusion of antigenic determinants not associated with protection that may unpredictably skew the immune response (27). With few exceptions, SARS vaccine formulations have not been tested against heterologous challenges in immunosenescent models of severe end stage lung disease (48).

Effective SARS vaccines must meet several criteria, including (i) the ability to protect against heterologous viral variants that arise during independent emergence events, since many S-targeted antibodies have significantly reduced neutralization titers against heterologous spike glycoproteins (11, 19, 44); (ii) the ability to elicit robust immune responses in elderly populations that are difficult to immunize and at increased risk for SARS-CoV-induced morbidity and mortality (14, 29); and (iii) avoidance of adverse vaccine outcomes, such as the vaccine-induced immune pathology that has been demonstrated following vaccination with the SARS N protein (11, 61). Whole inactivated SARS-CoV vaccines have demonstrated efficacy in young-animal models, generating high titers of neutralizing antibodies, yet most challenge studies have used a virus replication model devoid of clinical disease (17, 46, 50). In humans, inactivated SARS-CoV vaccines have been shown to induce neutralizing antibodies in healthy young subjects in phase 1 clinical trials (24, 28, 41). However, in neither humans nor animal models have inactivated vaccines been assessed for their ability to provide protection in aged populations or to protect against heterologous challenges. Given the severity of disease in aged populations and the possibility that emergent SARS viruses will be antigenically distinct from the 2002 epidemic strain, animal models that capture severe age-related disease and allow assessment of heterologous SARS challenges are essential for the preclinical validation of any vaccine or therapeutic candidate. The aged BALB/c mouse model reproduces age-related susceptibility to SARS-CoV disease similar to that noted in human infections, including increased levels of SARS-CoV replication, more severe clinical disease, and enhanced pulmonary histopathology (42, 45, 59). When challenged with zoonotic and human chimeric SARS-CoV incorporating variant spike glycoproteins, the aged BALB/c mouse model reproduces severe lung damage associated with human disease, including diffuse alveolar damage, hyaline membrane formation, and death, thereby also providing a model for assessing vaccine-mediated protection against heterologous viruses (45).

To test these hypotheses, we characterize the efficacy of an inactivated whole SARS-CoV vaccine in a highly lethal homologous and heterologous challenge model that recapitulates the age-related susceptibility and pathological findings seen in lethal human cases. The vaccine used was the CDC strain (AY714217) of SARS-CoV, doubly inactivated by formalin and UV irradiation, herein referred to as double-inactivated virus (DIV) (50). The vaccine had initially been characterized in tissue culture and young mice, where it was shown to induce neutralizing antibodies and to provide protection from viral replication. Adjuvanting with alum had minimal effect on the serum neutralizing titers or protection in these young-mouse protection studies (50). In this study, we chose to advance the protection and safety studies of DIV by assessing homologous and heterologous challenges in mice. We initially assess the vaccine's efficacy and potential for enhancement in a nonlethal animal model using icGD03-S. This synthetically derived virus incorporates the spike protein of a human strain isolated in 2004, providing a human virus challenge that is nonetheless divergent from the vaccine strain (45). Extending this protection study to the more stringent test of a lethal challenge, we utilize a mouse-adapted virus, icMA15, which is lethal in both young and old BALB/c mice and is minimally different from the vaccine strain (39). A chimeric virus incorporating the spike protein of a civet strain (HC/SZ/61/03) into the Urbani backbone provides a lethal heterologous and zoonotic challenge model (45). These three viral challenge regimens, varied adjuvants, and an aged-mouse model help to accurately model potential challenges of vaccinating a human population against future emergences involving a SARS-CoV-like zoonotic virus. Our results demonstrate vaccine-induced enhancement of eosinophilia and inflammatory response following challenge, as well as failure to protect against heterologous challenge in an aged-animal model. This work highlights the challenge of vaccine design for zoonotic viruses, the need for developing broadly neutralizing therapeutics, and the particular difficulty of immunizing aged populations and offers new routes for understanding SARS-CoV pathogenesis.

## MATERIALS AND METHODS

The generation and characterization of each of the recombinant infectious clones (icUrbani, icGD03-S, and icHC/SZ/61/03-S) have been described previously (45, 63). Briefly, all recombinant icSARS-CoV strains were propagated on Vero E6 cells in Eagle's minimal essential medium (MEM) (Invitrogen, Carlsbad, CA) supplemented with 10% fetal calf serum (HyClone, Logan, UT), kanamycin (0.25 μg/ml), and gentamicin (0.05 μg/ml) at 37°C in a humidified $CO_2$ incubator. All work was performed in a biological safety cabinet in a biosafety level 3 (BSL3) laboratory containing redundant exhaust fans. Personnel were equipped with powered air-purifying respirators with high-efficiency particulate air and organic vapor filters (3M, St. Paul, MN), wore Tyvek suits (DuPont, Research Triangle Park, NC), and were double gloved.

**Viruses and cells.** The icGD03-S (AY525636) (47), icMA15 (FJ882957), and icHC/SZ/61/03-S (45) strains of SARS-CoV were propagated on Vero E6 cells in Eagle's MEM supplemented with 10% fetal calf serum, kanamycin (0.25 μg/ml), and gentamicin (0.05 μg/ml) at 37°C in a humidified $CO_2$ incubator. For virus growth, cultures of Vero E6 cells were infected at an approximate multiplicity of infection (MOI) of 1 for 1 h, and the monolayer was washed twice with 2 ml of phosphate-buffered saline (PBS) and then overlaid with complete medium. At 30 h postinfection, the supernatant was clarified by centrifugation at 1,600 rpm for 10 min, aliquoted, and frozen at −70°C. Virus stocks were titrated by plaque assay.

**Mouse vaccination and challenge.** Due to the poor availability of aged mice, two slightly divergent mouse strains were utilized during the course of this research. BALB/c mice (Harlan Laboratoriess, Indianapolis, IN) were challenged with lethal viruses (icMA15 and icHC/SZ/61/03-S), while the National Institute of Aging (NIA) provided BALB/cBy mice for nonlethal/epidemic strain challenges. Prior studies in our laboratory have shown conserved susceptibility phenotypes in these mouse strains following SARS-CoV challenge, with slightly increased morbidity and mortality in the NIA (BALB/cBy) strain. Therefore, in

the nonlethal icGD03-S challenge, we expected slightly more morbidity than normally would have been predicted in Harlan mice.

Female BALB/cAnNHsd mice (young [6 to 8 weeks old] and aged [12 to 14 months old]; Harlan Laboratories, Indianapolis, IN) were separated into 4 groups of 12 young and 12 aged mice. The mice within each group were vaccinated by footpad injection with 20-μl volumes consisting of 0.2 μg of double-inactivated SARS-CoV vaccine, 0.2 μg of double-inactivated SARS-CoV vaccine with alum, 0.2 μg of inactivated influenza virus (iFlu), or 0.2 μg of inactivated influenza virus with alum. The mice were boosted with the same regimen 22 to 28 days later. Aged female BALB/cBy mice (12 to 14 months old; NIA) were vaccinated with PBS-, alum-, or VAP (VEE [Venezuelan equine encephalitis virus] replicon [VRP] adjuvanting particle)-adjuvanted iFlu ($n$ = 8, 10, and 9, respectively) or DIV ($n$ = 10, 9, and 10, respectively) immunogen. The vaccine formulations consisted of 0.2 μg of DIV or iFlu plus either PBS, 0.69 mg/ml alum, or $10^5$ infectious units (IU) of VAP, a dose which had previously been demonstrated to provide protective immunity in young mice (25, 54). These mice were then boosted with the same regimen 22 to 28 days later.

We collected blood from tail veins prior to challenge with icMA15, icHC/SZ/61/03, or icGD03-S on day 36 postvaccination. Mice were anesthetized with a ketamine (1.3 mg/mouse)-xylazine (0.38 mg/mouse) mixture administered intraperitoneally in a 50-μl volume. The mice were intranasally inoculated with $10^5$ PFU of icMA15, icHC/SZ/61/03, or icGD03-S in 50-μl volumes and weighed daily. At 2 or 4 days postinfection, the mice were euthanized with isoflurane, and lung and serum samples were collected for analysis. For studies involving VRP vaccinations, 5-week-old female BALB/c mice were immunized with $10^5$ IU of VRPs expressing SARS-CoV N, a bat coronavirus (BtCoV.279) N, or hemagglutinin (HA) in a 10-μl volume by footpad injections. Three weeks later, blood was collected by the tail nick method for enzyme-linked immunosorbent assay (ELISA), and the mice were boosted with $10^5$ IU of the respective VRPs. Three weeks postboost, blood was collected by tail nick for assessing antibody responses. The mice were moved to a satellite facility under BSL3 conditions, acclimatized, and challenged with $10^5$ PFU of recombinant MA15 (rMA15) icGDO3 virus (48) by intranasal inoculation as described above.

All mice were housed under sterile conditions in individually ventilated Sealsafe cages using the SlimLine system (Tecniplast, Exton, PA). Experimental protocols were reviewed and approved by the Institutional Animal Care and Use Committee at the University of North Carolina, Chapel Hill, NC.

**Plaque assay titration of virus from lungs.** One-quarter of each lung was taken for determination of the viral titer. Samples were weighed and homogenized for 60 s at 6,000 rpm in four equivalent volumes of PBS to generate a 20% solution. The solution was centrifuged at 13,000 rpm under aerosol containment in a table top centrifuge for 5 min, the clarified supernatant was serially diluted in PBS, and 200-μl volumes of the dilutions were placed onto monolayers of Vero E6 cells in six-well plates. Following 1 h of incubation at 37°C, the cells were overlaid with 0.8% agarose-containing medium. Two days later, the plates were stained with neutral red, and the plaques were counted.

**Plaque reduction neutralization titer assays.** We heat inactivated mouse serum at 55°C for 30 min and then serially diluted it to 1:50, 1:100, 1:200, 1:400, and 1:800 in PBS to a volume of 125 μl. Next, we added 125 μl of PBS containing 125 PFU of icSARS-CoV to each serum dilution, incubated the virus-serum mixtures at 37°C for 30 min, added 200 μl of each mixture to confluent cultures of Vero E6 monolayers, and allowed them to incubate at 37°C for 1 hour. Following the 1-h infection, we covered each monolayer with 4 ml of 0.8% agarose melted in standard Vero E6 cell medium and resolved the plaques with neutral red staining 2 days later. Finally, we calculated the 50% plaque reduction neutralization titer ($PRNT_{50}$) values, the serum dilutions at which plaque formation was reduced by 50% relative to that of virus not treated with serum.

**Lung histopathology.** One-half of each lung was fixed in 4% paraformaldehyde (PFA) in PBS (pH 7.4) for at least 7 days, embedded in paraffin, sectioned to 5 μm, and stained with hemotoxylin and eosin (H&E). Sections were blindly evaluated by W. Funkhouser for the extent of tissue damage and characterization of inflammation.

**Visual enumeration of eosinophils.** Lung tissues were prepared as described above and stained with H&E or Congo red (plus hematoxylin) (30). For each slide, an initial assessment of gross lung pathology was followed by selection of a lung section and enumeration of eosinophils within the viewing field at ×400 magnification. Representative images were minimally and identically processed to enhance contrast in Adobe Photoshop CS4. For both H&E- and Congo red-stained slides, multiple 160-$\mu m^2$ sections proximate to airways were assessed, and the eosinophils counted were averaged per lung.

**Quantitative real-time reverse-transcription (RT)-PCR.** One-quarter of a lung from each mouse was placed into RNAlater (Ambion) for 4 days at 4°C and then frozen at −70°C. Lung samples were transferred from RNAlater to TRIzol and homogenized for 60 s at 6,000 rpm, and RNA was extracted by chloroform/isopropanol precipitation. cDNA was prepared by standard protocols using random hexamers and SuperScript II Reverse Transcriptase (Invitrogen). Quantitative PCR was conducted on a Lightcycler 480II (Roche) using ABI TaqMan Gene Expression Assays specific for mouse GAPDH (glyceraldehyde-3-phosphate dehydrogenase) or mouse interleukin 4 (IL-4), IL-5, gamma interferon (IFN-γ), IL-13, CCL11 (eotaxin), or Cxcl1 Keratinocyte-derived chemokine (KC). Relative quantification was calculated as the $\log_{10}$ fold change ($2^{\Delta\Delta CT}$) relative to mock-vaccinated, mock-challenged controls.

**Flow cytometry.** Mice vaccinated with PBS, DIV, or DIV plus alum were challenged with $10^5$ PFU of icHC/SZ/61/03, weighed and monitored daily for morbidity, and euthanized 4 days postinfection by isoflurane inhalation. The lungs were perfused with 10 ml PBS by cardiac puncture, dissected, manually minced, and vigorously agitated for 2 h in digestion medium (RPMI, 10% fetal bovine serum [FBS], 15 mM HEPES, 1.7 mg/ml DNase 1 [Sigma], 2.5 mg/ml collagenase A [Roche], 1× streptomycin, 1× gentamicin). The lungs were then passed through a 75-μm cell strainer, resuspended in RPMI medium (RPMI, 10% FBS, 15 mM HEPES), and overlaid on a density gradient of iodixanol diluted to a density of 1.079 $gm/cm^3$ with RPMI 1640 containing 10% FBS (Optiprep, Sigma-Aldrich Co., St. Louis, MO). Following centrifugation, cells were collected from the interface and washed, and viable cells were counted with a Countess automated cell counter (Invitrogen). The cells were then incubated with the following panel of antibodies: allophycocyanin (APC) anti-leukocyte common antigen (LCA), PE-Cy7 anti-CD11b, and phycoerythrin (PE)-Cy5 anti-major histocompatibility complex (MHC) class II antigens, all from eBioscience (San Diego, CA); fluorescein isothiocyanate (FITC) anti-Gr-1 and PE anti-SiglecF, from BD-Pharmingen (San Diego, CA); and PE-Texas Red anti-CD11c (Molecular Probes Invitrogen, Carlsbad, CA). Following staining, the cells were washed with fluorescence-activated cell sorter (FACS) wash buffer (1× Hanks balanced salt solution [HBSS], 1% FBS) and fixed with 2% formalin, and flow cytometry was conducted on a CyAn ADP (Beckman-Coulter) with 300,000 live-cell events gathered per lung sample. Analysis was performed with Summit software (version 5.2; Beckman-Coulter). First, we gated on $LCA^+$ and $CD11c^+$ cells by plotting those parameters against forward scatter and gating on positive cells. Then, Gr-1 was plotted against SigLecF (see Fig. 8A). SigLecF-high, Gr-1-intermediate cells were selected, and CD11b signal versus CD11c signal was plotted for cells in that region. $CD11b^+$, $CD11c^-$ cells are classified as eosinophils, while alveolar macrophages are $CD11c^+$ (see Fig. 8b). After gating on $LCA^+$ and $CD11c^+$ cells, Gr-1-positive cells are classified as neutrophils (see Fig. 8a). Of the cells that remain after gating out $SiglecF^+$ cells and neutrophils, we classify MHC class II-negative, $CD11b^+$, and B220-negative cells as monocyte-derived dendritic cells (mDCs). The cell counts per lung were calculated as the product of the total viable lung cell population by the percentage of gated cells in live-cell events. We used a two-factor analysis of variance (ANOVA) to assess the statistical significance of age and vaccine on the overall number of cells. If the ANOVA determined a factor was significant, *post hoc* analyses using Tukey's honestly significant differences (HSD) were used to further determine the effects of treatment on cell counts.

**Enzyme-linked immunosorbent assay.** Antigen-specific IgG and IgG subisotype titers were determined by ELISA. Briefly, purified recombinant SARS N protein or S protein was coupled to high-binding 96-well ELISA plates (Greiner) in basic carbonate buffer (pH = 9.6). After washing with ELISA wash buffer (EWB) (PBS with 0.016% Tween 20), diluted serum was added to the wells in EWB with 10% blocking buffer (Sigma-Aldrich). After 2 h at 4°C, the plates were washed again, and horseradish peroxidase-conjugated goat anti-mouse IgG, IgG1, or IgG2a was added to the appropriate wells diluted in EWB plus blocking buffer. After another 2 h, chromogenic substrate (*o*-phenylenediamine in citrate buffer with added hydrogen peroxide) was added to each well. After 30 min, the reaction was stopped with the addition of 0.1 M sodium fluoride and read at 450 nm. A sigmoidal curve was fit to each set of optical density (OD) versus $\log_{10}$ serum dilution values using the curve-fitting software of the SigmaPlot graphics package (Systat Software, Inc.), and the inflection point (where the OD is one-half of the maximum value recorded for that isotype-antigen combination) is calculated and reported as the "half-max titer."

## RESULTS

**DIV provides partial protection against nonlethal heterologous challenge in aged animals.** The efficacy of double-inactivated SARS-CoV vaccines has not been evaluated in aged animals, which show immunosenescence, increased suscepti-

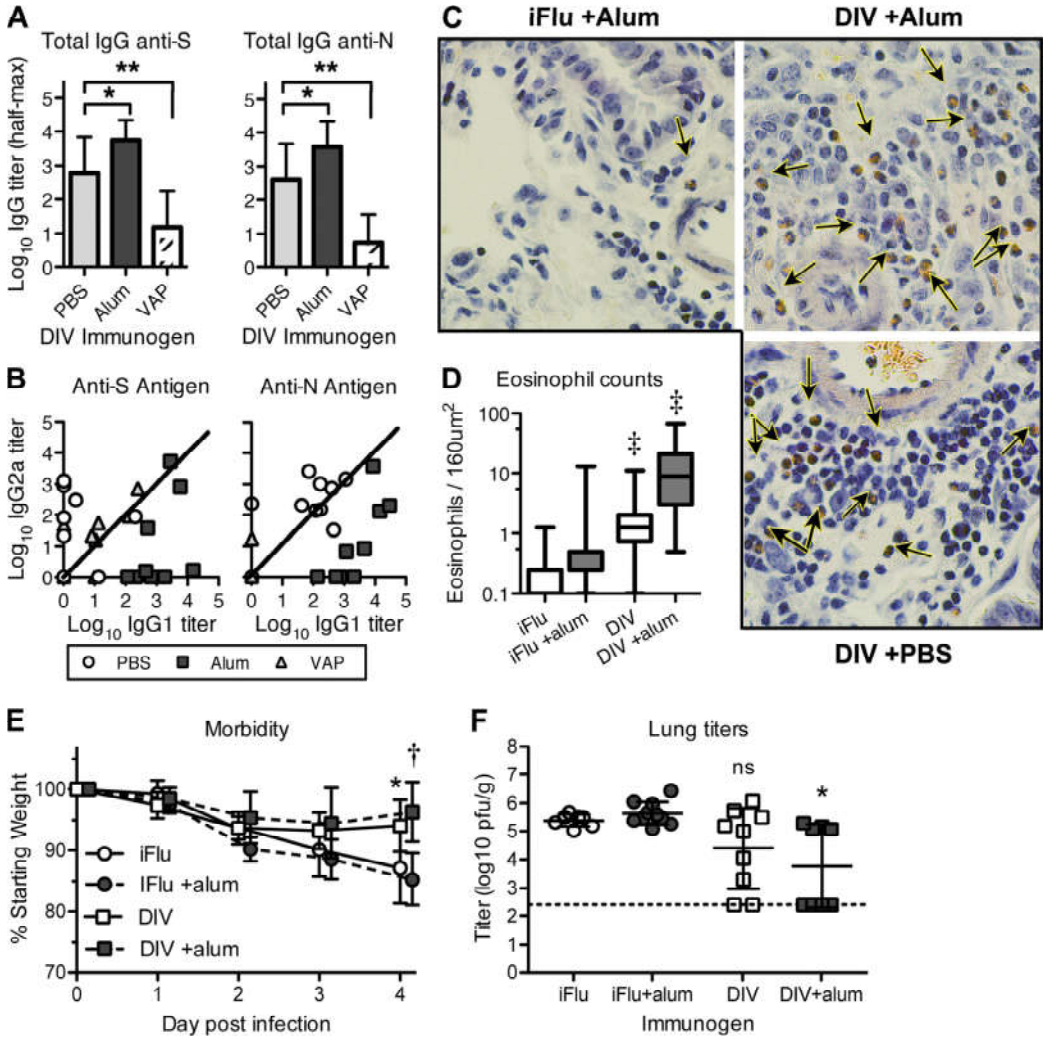


FIG. 1. DIV vaccination and nonlethal heterologous challenge in aged animals. (A) $Log_{10}$ half-maximum ELISA titers for anti-N and anti-S total IgG antibodies following DIV immunization. One-year-old aged NIA mice were immunized with DIV ($n = 10$), DIV plus alum ($n = 9$), or DIV plus VAP ($n = 9$). The values were statistically compared by a Mann-Whitney test. The error bars indicate standard deviations. (B) $Log_{10}$ half-maximum ELISA titers of IgG1 versus IgG2a subtypes. Each point represents $log_{10}$ IgG1 and IgG2a half-max titers for a single mouse. (C) Representative images (×400 magnification) of eosinophil infiltration in icGD03-S-challenged mice following DIV or iFlu vaccination regimens. Lungs taken 4 days postinfection were sectioned and stained with Congo red, a reliable and specific stain for eosinophils (arrows). (D) Box and whisker counts of eosinophils proximal to airways in icGD03-S-challenged aged mice, with the range shown by the whiskers. Eosinophils were counted in 4 160-$\mu m^2$ regions proximal to airways (5 airways per mouse). The counts were statistically compared to those of adjuvanted controls by a *t* test with Welch's correction. (E) Mice challenged with the icGD03-S virus were weighed daily and visually assessed for morbidity. DIV and DIV-plus-alum immunogens significantly reduced the morbidity associated with icGD03-S challenge by day 4 postchallenge. (F) Mice were harvested on day 4, and one-quarter of the lung was homogenized, with the titer determined by plaque assay. Lung titers were sporadically reduced for both the DIV and DIV-plus-alum groups, with only DIV plus alum reaching statistical significance by the Mann-Whitney test. *, $P < 0.05$; **, $P < 0.01$; †, $P < 0.001$; ‡, $P < 0.0001$.

bility to clinical disease, and increased pathology, reflecting conditions in the more vulnerable SARS-CoV-infected aged populations (48, 50). One-year-old National Institute of Aging mice were vaccinated with double-inactivated SARS vaccine (DIV) or nonspecific immunogen (iFlu) in unadjuvanted form, adjuvanted with alum, or adjuvanted with VAP. SARS-specific total IgG responses, as measured by ELISA, show a significant increase in the alum-adjuvanted group compared to the PBS-adjuvanted group for both N-specific (3.580 versus 2.625 $log_{10}$ half-max titer) and S-specific (3.743 versus 2.781 $log_{10}$ half-max titer) antibodies (Fig. 1A). Unexpectedly, the VAP adjuvant nearly ablated total IgG antibody compared to PBS, reducing total S- and N-specific antibodies to titers of 0.7432 and 1.182 $log_{10}$ half-max, respectively (Fig. 1A). The alum-adjuvanted DIV induced a strong skew in the N- and S-specific antibodies toward IgG1, a subtype associated with Th2 immune responses, while the nonadjuvanted DIV resulted in a more balanced or IgG2a-skewed antibody population (Fig. 1B).

To assess protection from heterologous SARS infection, the aged DIV-vaccinated mice were challenged with $10^5$ PFU of icGD03-S, a recombinant heterologous human strain that closely resembles zoonotic strains circulating in 2004. Both DIV- and DIV-plus-alum-vaccinated groups showed significant, though incomplete, reductions in morbidity (as measured

by weight loss) by day 4 postinfection, while none of the nonspecific-vaccination groups showed any reduction in morbidity or lung viral titer by 4 days postinfection (Fig. 1E and F). The VAP-adjuvanted DIV group predictably showed no reduction in morbidity or titer, consistent with the failure of DIV plus VAP to induce SARS-specific antibody responses in the aged animals (data not shown). When the viral titers in the lungs were assessed, only the DIV-plus-alum group showed significant reductions in day 4 lung titers, while all other groups, including non-adjuvanted DIV, showed high levels of viral replication (Fig. 1F). These results demonstrate that while DIV does provide some heterologous protection in highly susceptible aged populations, the vaccine is unable to provide complete protection from either viral replication or virus-induced morbidity.

Previous work by our group and others has demonstrated that vaccination with SARS N protein fails to protect from SARS replication while driving a vaccine-induced eosinophilic pathology. Therefore, given that none of the DIV vaccine strategies resulted in complete protection from viral replication in the aged animals, we assessed whether any of the vaccine groups exhibited signs of eosinophilic immune pathology. Importantly, both the DIV and DIV-plus-alum groups showed increased numbers of eosinophils in the lungs following challenge (Fig. 1C). Mice vaccinated with iFlu and iFlu-plus-alum showed a low number of eosinophils in regions proximate to airways by Congo red staining: both iFlu and iFlu-plus-alum groups had a median count of 1.0 eosinophil per region (Fig. 1D). Both DIV- and DIV-plus-alum-vaccinated groups showed significant increases in eosinophil counts over the comparable nonspecific immune groups at 5.0 and 35.0 eosinophils per region, respectively. Further, adjuvanting with alum significantly increased the eosinophil influx compared to DIV alone.

**Immunization of young and aged animals.** Few candidate vaccines have been tested in aged animals following homologous and heterologous lethal challenge, and no whole-virus vaccines have been so tested. Therefore, we assessed whether the DIV formulations would protect against heterologous and homologous lethal challenges in young- and aged-animal models. As a control, vaccination with inactivated influenza virus with or without alum did not induce detectable levels of anti-SARS (Urbani) antibody in either 12-week-old young or 59-week-old aged mice (data not shown). When young mice were vaccinated with 0.2 μg of the SARS-CoV DIV, 8/16 generated detectable levels of SARS neutralizing antibody titers. Vaccination with DIV plus alum induced detectable levels of neutralizing antibody in 15/15 mice and at significantly increased PRNT levels compared to DIV alone (Fig. 2). Specifically, the mean (±standard deviation [SD]) $PRNT_{50}$ value for DIV alone was 221 ± 220, which significantly differed from the DIV-plus-alum group's neutralizing titer of 2,710 ± 992 (Fig. 2). Importantly, DIV alone did not induce detectable levels of anti-SARS antibodies in aged mice, while the addition of alum increased the response in aged animals, with 8/14 aged animals generating detectable levels of neutralizing antibodies. The mean $PRNT_{50}$ value was 425 ± 806, significantly reduced by about 6-fold compared with DIV-plus-alum-vaccinated young animals. Thus, in young and aged animals, the presence of alum in the DIV vaccine formula significantly improved the induction of SARS-CoV neutralizing antibody: from moderate to high levels in young animals and from unmeasurable to moderate levels in aged animals.

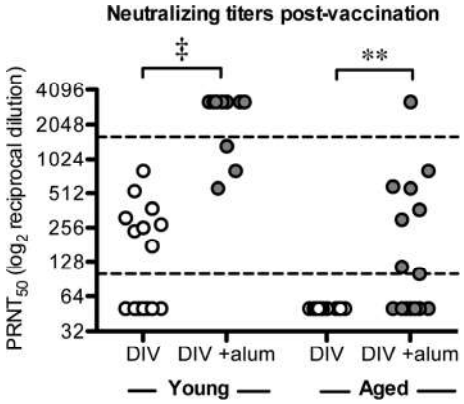


FIG. 2. Neutralizing antibody titers of vaccinated mice. Shown are $PRNT_{50}$ values of sera collected from young and aged mice vaccinated with DIV or DIV plus alum. Neutralizing titers were significantly reduced in both aged vaccination groups compared to the young groups (DIV, $P < 0.01$; DIV plus alum, $P < 0.0001$; Fisher exact test). Alum adjuvant significantly increased neutralization titers for both young and aged animals (**, $P < 0.01$; ‡, $P < 0.0001$; 2-tailed Mann-Whitney test). No neutralizing antibody was detectable for young or aged mice vaccinated with iFlu ($n = 15$ and $n = 16$, respectively) or iFlu plus alum ($n = 14$ and $n = 15$, respectively) (data not shown). $PRNT_{50}$ values below the limit of detection were assigned a value of 50 and those above the upper limit of quantification (ULOQ) a value of 3,200. (lower limit of quantification [LLOQ] = 100; ULOQ = 1,600).

**Lethal mouse-adapted and zoonotic challenges in young mice.** To directly assess vaccine-mediated protection from lethal disease in young and old animals, mice were challenged either with the homologous mouse-adapted icMA15 virus or with the heterologous zoonotic virus icHC/SZ/61/03-S. In young animals, DIV provided partial protection, increasing survival following challenge with icMA15 from 0% to 83.3% and significantly reducing morbidity by day 3 ($P < 0.01$; 2-tailed Mann-Whitney test). In contrast, DIV plus alum provided complete protection from morbidity and mortality by 4 days postinfection in icMA15-challenged mice (Fig. 3A and B). When young mice were challenged with icHC/SZ/61/03-S, both the DIV alone and DIV-plus-alum groups were provided complete protection from mortality. The DIV-plus-alum group showed complete protection from morbidity, while DIV-immunized groups showed mild weight loss. The nonspecifically vaccinated groups (iFlu and iFlu-plus-alum) lost ~20% of their starting weight by day 3 (icMA15) or day 4 (icHC/SZ/61/03-S) postinfection, respectively. Furthermore, the iFlu- and iFlu-plus-alum-vaccinated icMA15-infected animals showed 0% survival by day 4, while the same groups challenged with icHC/SZ/61/03-S showed 67% and 50% survival, respectively. In short, although DIV-mediated protection was not complete, there was partial protection from homologous and heterologous lethal challenges in young animals, and this protection from weight loss and death was enhanced by the inclusion of alum adjuvant.

When viral titers were assessed in the lungs at day 4 postinfection, young mice vaccinated with DIV plus alum showed no detectable viral titer following either viral challenge (Fig. 3C).

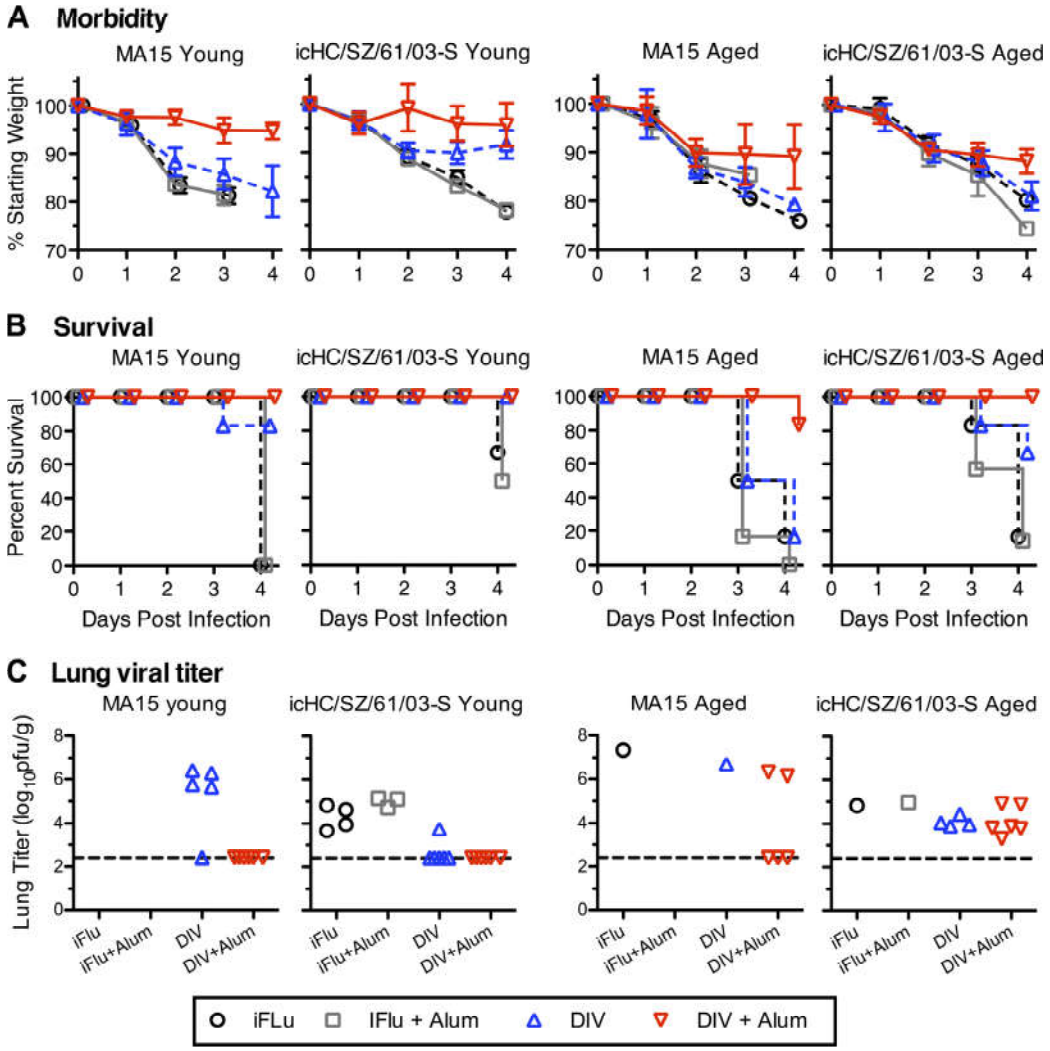


FIG. 3. Morbidity and mortality of lethal mouse-adapted and zoonotic challenges following DIV immunization. (A and B) Young and aged mice were vaccinated with iFlu, iFlu plus alum, DIV, or DIV plus alum ($n$ = 6 per group) and subsequently mock infected (data not shown) or challenged with $10^5$ PFU of icMA15 or icHC/SZ/61/03-S. The mice were weighed daily and monitored for morbidity (A) and mortality (B). (C) Four days postinfection, lungs were harvested, and the viral load was assessed by plaque assay. Values were statistically compared by Mann-Whitney test. The error bars indicate standard deviations.

In contrast, for DIV alone, lung titers following icMA15 challenge were reduced to undetectable levels in only 1 of 5 surviving mice, and the remaining 4 had titers ranging from 5.65 to 6.41 $\log_{10}$ PFU/g. Following icHC/SZ/61/03-S challenge, viral titers in DIV-vaccinated mice were reduced to undetectable levels for all but 1 mouse (3.74 $\log_{10}$ PFU/g). In comparison, the iFlu-immunized groups had titers ranging from 3.65 to 4.83 $\log_{10}$ PFU/g (iFlu) and 4.72 to 5.14 $\log_{10}$ PFU/g (iFlu plus alum). Therefore, in agreement with morbidity data, DIV plus alum was able to provide complete protection in young animals, while DIV alone reduced but did not eliminate viral replication following homologous or heterologous challenge.

**Lethal mouse-adapted and zoonotic challenges in aged mice.** In stark contrast to the encouraging results seen in young animals, 1-year-old aged animals vaccinated with either DIV alone or DIV-plus-alum did not show complete protection from mortality, and both groups demonstrated significant morbidity, with weight loss and high levels of viral replication. As in young animals, iFlu-vaccinated groups showed an ~20% weight loss by day 3 (icMA15) or 4 (icHC/SZ/61/03-S) postinfection. Survival following icMA15 challenge was 16.7% and 0% on day 4 for iFlu and iFlu-plus-alum, respectively; following icHC/SZ/61/03-S challenge, the rate was 16.7% for each treatment. Unlike young animals, aged groups vaccinated with DIV alone did not show promising reductions in morbidity, mortality, or viral titer following these lethal challenges (Fig. 3). icMA15- or icHC/SZ/61/03-S-challenged groups vaccinated with DIV alone had greater than 20% weight loss by day 4, and the DIV immunization provided no significant increases in survival for either virus challenge (16.7% for icMA15 and 66.7% for icHC/SZ/61/03-S). The one surviving mouse following icMA15 challenge had a lung viral titer of 6.70 $\log_{10}$ PFU/g, and following icHC/SZ/61/03-S challenge, the surviving mice had lung titers ranging from 3.89 to 4.44 $\log_{10}$ PFU/g, which was slightly reduced compared to the peak titers seen in surviving iFlu-vaccinated control mice (4.83 and 4.98 $\log_{10}$ PFU/

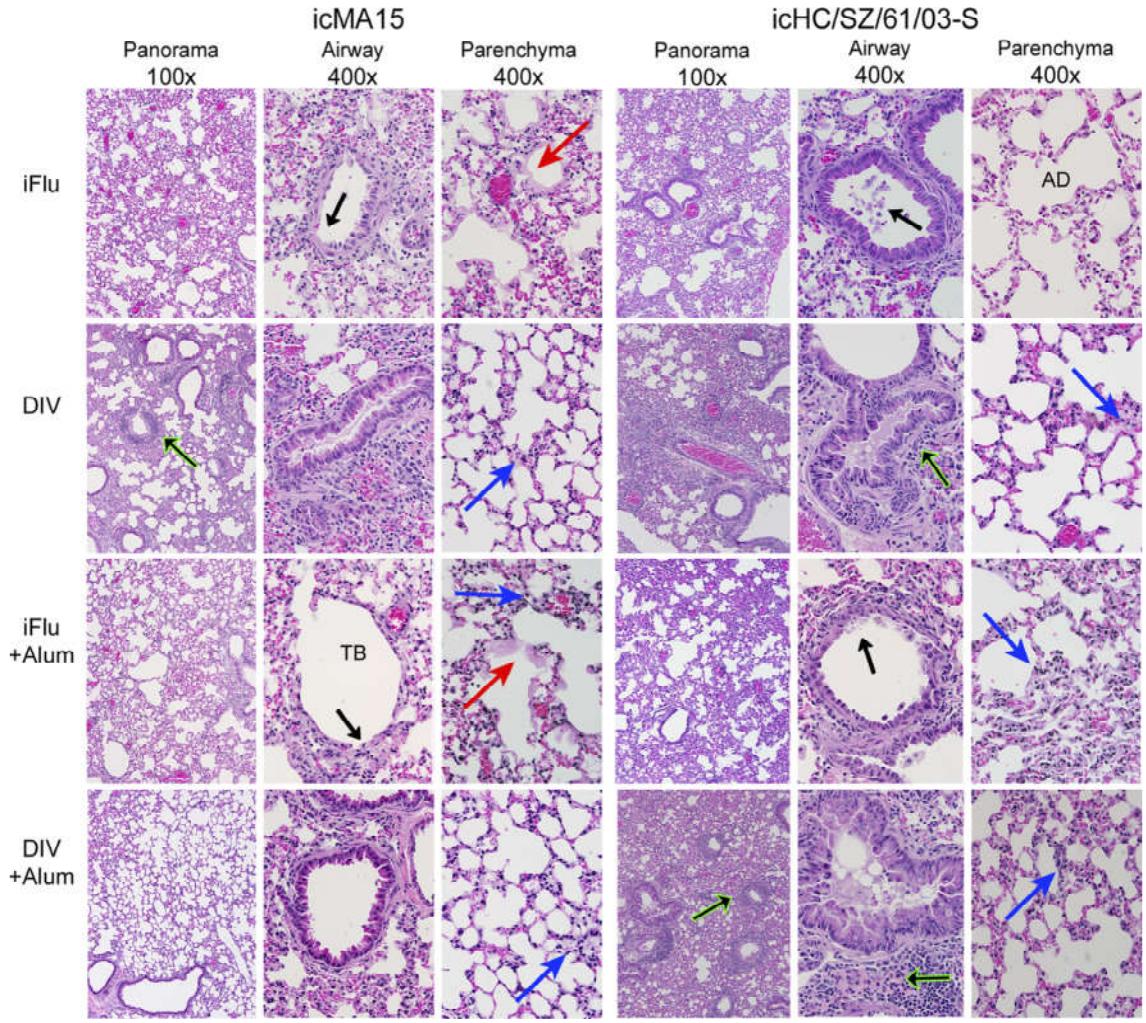


FIG. 4. Pathology in young mice challenged with icMA15 or icHC/SZ/61/03-S. Shown are representative images of H&E-stained lung panorama (×100), airway (×400), and parenchyma (×400) sections from young mice vaccinated with the indicated immunogen and challenged with icMA15 or icHC/SZ/61/03-S. TB, terminal bronchiole; AD, alveolar duct; black arrows, denuded airway; blue arrows, acute alveolitis and septal congestion; green arrows, peribronchovascular cuffing; red arrows, hyaline membrane.

g). In contrast to DIV alone, DIV plus alum did significantly increase survival rates for aged mice after both icMA15 and icHC/SZ/61/03-S challenges compared to the iFlu-plus-alum-immunized groups. Following icMA15 challenge, aged mice vaccinated with DIV plus alum showed 83.3% survival by day 4 (versus 0% for iFlu plus alum; $P < 0.01$; 2-tailed Fisher exact test), and the comparable group challenged with icHC/SZ/61/03-S showed 100% survival (versus 16.7% for iFlu plus alum; $P < 0.01$; 2-tailed Fisher exact test). However, mice in both the icMA15- and icHC/SZ/61/03-S-challenged groups had significant weight loss compared to mock-infected controls ($P < 0.05$ for both) (Fig. 3A). Additionally, DIV plus alum reduced lung titers to undetectable levels by day 4 in only 3 of the 5 surviving icMA15-challenged animals and did not eliminate virus from any of the surviving icHC/SZ/61/03-S-challenged animals despite 100% survival in those animals (Fig. 3C).

**Pathological findings in icMA15- or icHC/SZ/61/03-S-challenged animals.** DIV alone failed to provide complete protection from SARS replication and disease in both young and old animals, while DIV plus alum failed to prevent weight loss in aged animals, suggesting that neither vaccine formulation would protect from SARS-induced respiratory pathology. We therefore evaluated the lungs of animals from each of the vaccination groups for vaccine-induced pathology. Lethal challenges to naïve mice result in a denuding bronchiolitis and apoptotic debris in the airways of both young and old animals. Young mice challenged with icHC/SZ/61/03-S displayed diffuse parenchymal alveolitis, while challenge with icMA15, and both challenges to aged mice, demonstrated additional pathology, including diffuse alveolar damage (DAD) and hyaline membrane formation, both hallmarks of acute respiratory distress syndrome (ARDS) in SARS cases (young, Fig. 4; aged, Fig. 5).

Young animals vaccinated with DIV suffered significant pathological changes that were generally worse in icMA15- than icHC/SZ/61/03-S-challenged animals. Compared to mock-vaccinated groups, the DIV-vaccinated groups showed increased perivascular and peribronchial cuffing, as well as scattered infiltrates in the parenchyma, including neutrophils, alveolar macrophages, and eosinophils (Fig. 4). DIV-vaccinated aged animals showed greater pathology than young an-

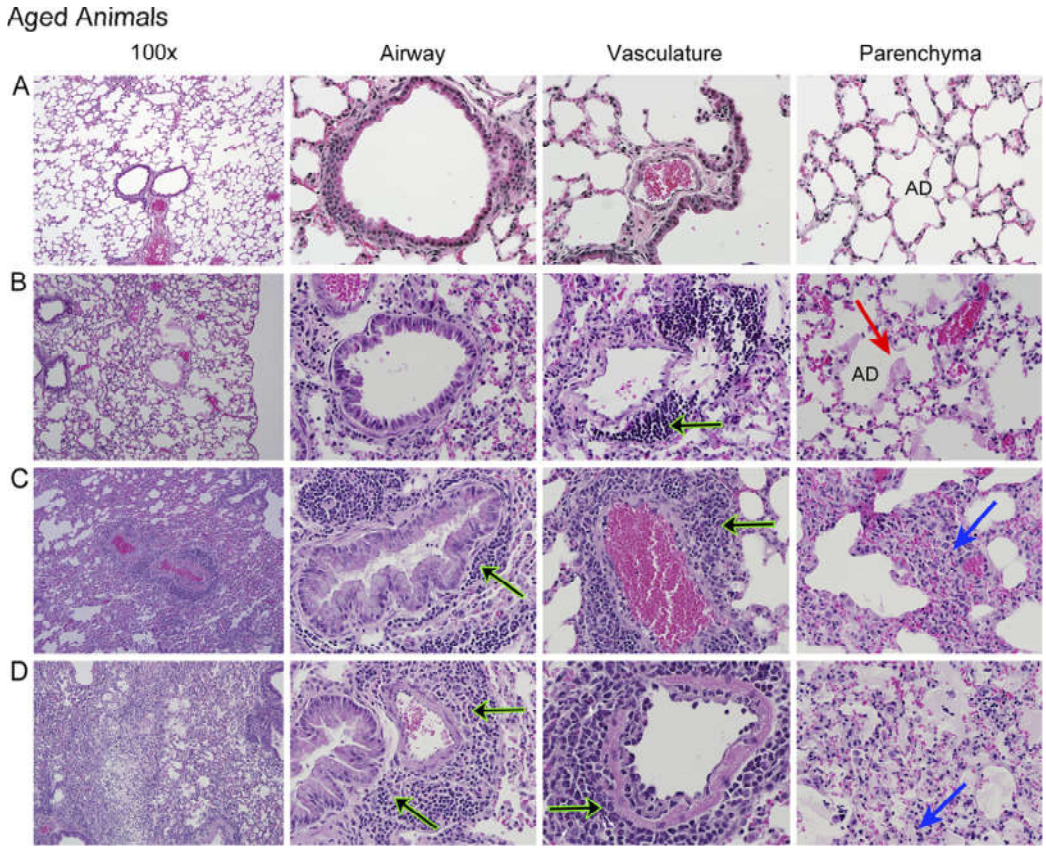


FIG. 5. Pathology following immunization and subsequent lethal challenge in aged Harlan mice. Shown are representative H&E-stained sections of panorama (×100), airway (×400), vasculature (×400), and parenchyma (×400) lung regions from aged mice: (A) mock infected; (B) iFlu plus alum vaccinated, icHC/SZ/61/03-S challenge; (C) DIV plus alum vaccinated, icHC/SZ/61/03-S challenge; (D) DIV plus alum vaccinated, icMA15 challenge. See the legend to Fig. 4 for arrow definitions.

imals, particularly perivascular cuffing and interstitial thickening (Fig. 5). These results indicate that not only did the DIV vaccine fail to protect from viral replication and morbidity/mortality, but the vaccine actually promoted the development of enhanced inflammatory damage within the lungs.

The adjuvanted vaccine, DIV plus alum, well protected young mice from icMA15 challenge, showing minimal pathological changes. However, despite good protection from weight loss or lethality, DIV-plus-alum icHC/SZ/61/03-S-challenged mice showed histopathology more extensive than that in unvaccinated mice, with increased peribronchiovascular cuffing consisting of mature lymphocytes, macrophages, and eosinophils (Fig. 4). In aged animals, DIV plus alum provided little protection against either challenge, demonstrating pathology beyond that in the unvaccinated mice, with additional perivascular and peribronchial cuffing, as well as fibrinous exudates in the alveolar parenchyma (Fig. 5C and D).

**Aged animals have increased Th2 effector and eosinophil-associated cytokine mRNA.** Given the Th2-associated skew in antibody profiles (Fig. 2) and the broad influx of inflammatory cells in vaccinated mice (Fig. 4 and 5), we used quantitative RT-PCR to analyze *in vivo* cytokine mRNA expression following vaccination and challenge (Fig. 6). Aged mice vaccinated with DIV plus alum and challenged with icHC/SZ/61/03 had elevated mRNA levels of Th2 effector cytokines, including IL-13 and IL-5, at 2 and 4 days postinfection ($P < 0.01$ for each). The eosinophil chemoattractant CCL11 (eotaxin) was significantly increased in the lungs of vaccinated mice at both 2 and 4 days postinfection ($P < 0.01$). In contrast, IL-4 and IFN-γ showed no significant changes at these time points (the earliest of which is day 2), and the neutrophil-associated chemokine, Cxcl1, was elevated in mock-vaccinated rather than DIV-vaccinated groups ($P < 0.05$).

**Vaccination and lethal challenge induce an eosinophilic pulmonary influx.** The presence of high numbers of eosinophils among the inflammatory infiltrates following vaccination and subsequent challenge has been a consistent observation associated with respiratory syncytial virus (RSV)- and measles vaccine-induced immunopathology and was observed in vaccination experiments with the SARS-nucleocapsid immunogen, peaking at 4 days postinfection (11, 61). To assess the eosinophilic influx following whole-virus immunization and lethal challenge, we blindly assessed H&E-stained lung sections of aged mice challenged with HC/SZ/61/03-S and enumerated eosinophils proximate to airways. Representative images (×400 magnification) of regions proximate to airways are shown in Fig. 7A, with counts of eosinophils per 160 $\mu m^2$ in Fig. 7B. A median 9.0 eosinophils per 160 $\mu m^2$ were present around the airways of DIV-vaccinated groups, comparable to the median 11.0 present in DIV-plus-alum groups. These

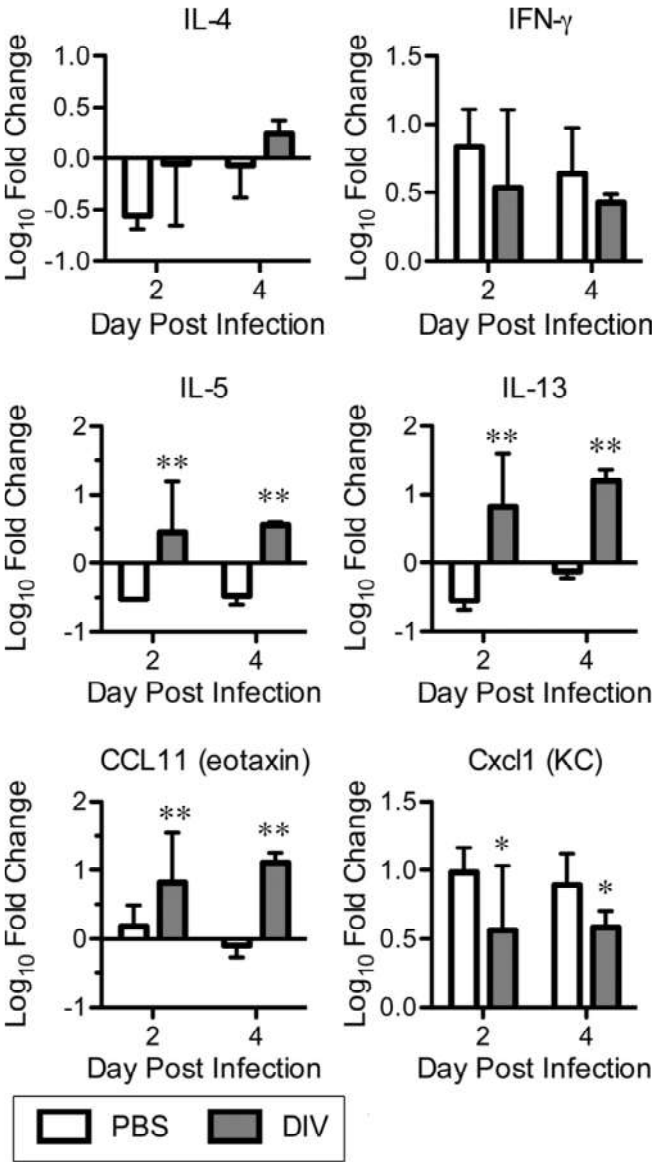


FIG. 6. Cytokine and chemokine mRNA expression profiles in aged mice. RNA was taken from the lungs of aged mice vaccinated with DIV plus alum and challenged with icHC/SZ/61/03 at 2 and 4 days postinfection. Cytokine and chemokine mRNAs were measured by quantitative real-time RT-PCR. The values are shown as $\log_{10}$ fold change over an unvaccinated, unchallenged control. *, $P < 0.05$; **, $P < 0.01$. The error bars indicate standard deviations.

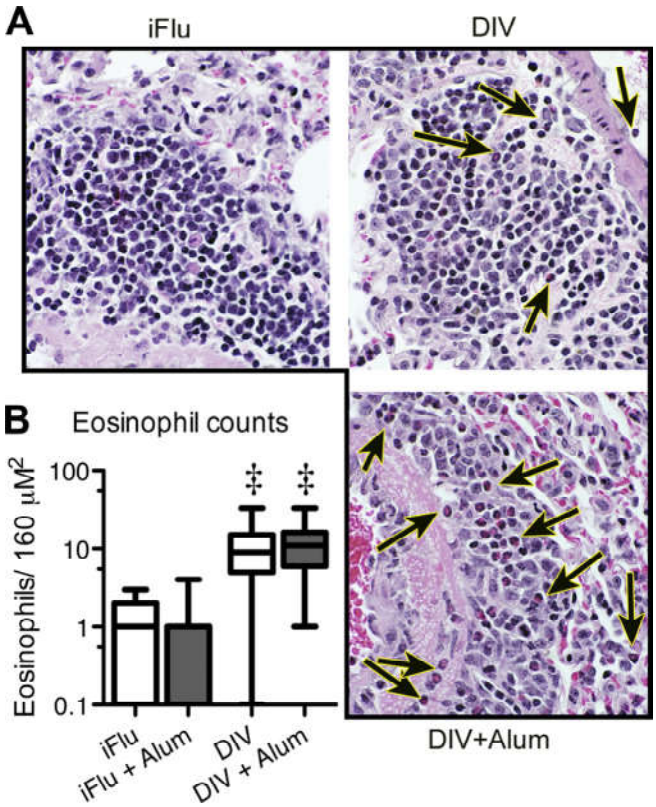


FIG. 7. Visual identification of eosinophils following lethal challenge. Eosinophils proximal to airways were counted in H&E-stained sections of lung from aged icHC/SZ/61/03-S-infected mice. (A) Representative images of regions counted, with eosinophils highlighted by arrows. (B) Box and whisker counts of eosinophils proximal to airways in icGD03-S-challenged aged mice, with ranges shown by the whiskers. Eosinophils were counted in 4 160-$\mu m^2$ regions proximal to airways; $n = 31$ fields per group. Both DIV- and DIV-plus-alum-immunized mice had visibly more eosinophils present following challenge than the nonspecific-immunogen groups. ‡, $P < 0.0001$; $t$ test with Welch's correction.

counts are significantly higher than in the iFlu (median, 1.0) and iFlu-plus-alum (median, 0.0) groups, respectively (Fig. 7B). These data suggested that increased eosinophilia occurs following DIV and DIV-plus-alum vaccination in young and aged animals, especially following heterologous challenge.

To precisely characterize the inflammatory infiltrate following DIV vaccination, we challenged PBS-, DIV-, or DIV-plus-alum-immunized young and aged mice with icHC/SZ/61/03-S and examined whole lungs by flow cytometric analysis at 4 days postinfection. Eosinophils, defined as $LCA^+$ $SiglecF^+$ $CD11b^+$ $CD11c^-$ populations (Fig. 8), were significantly increased in all vaccinated compared to unvaccinated populations following lethal challenge (Fig. 8A [$F_{2,32} = 14.739$; $P < 1 \times 10^{-4}$] and 9A). *Post hoc* analysis using Tukey's HSD showed that both DIV ($P = 0.0003433$) and DIV-plus-alum ($P < 1 \times 10^{-4}$) groups had significantly increased numbers of eosinophils compared to PBS-immunized animals. Adjuvant had no measurable effect on the eosinophilic influx, as DIV- and DIV-plus-alum-immunized mice did not have statistically significant differences in their overall numbers of eosinophils in either age group. Importantly, the elevated eosinophil counts were comparable between young and aged populations despite divergent clinical presentations. Further analysis of the inflammatory cell infiltrates of vaccinated mice showed a strong influence of age on the neutrophil ($F_{1,32} = 22.0339$; $P < 1 \times 10^{-4}$) and monocytic dendritic cell ($F_{1,32} = 26.681$; $P < 1 \times 10^{-4}$) influx, with both cell populations significantly increased in aged relative to young animals (Fig. 9B and D). Alveolar macrophage counts showed no significant differences compared to mock-vaccinated mice in either young or aged animals (Fig. 9C). Finally, the vaccinated animals showed significantly lower monocytic DC counts by day 4 postchallenge, independent of age ($F_{2,32} = 11.18$; $P = 0.0002079$), and *post*

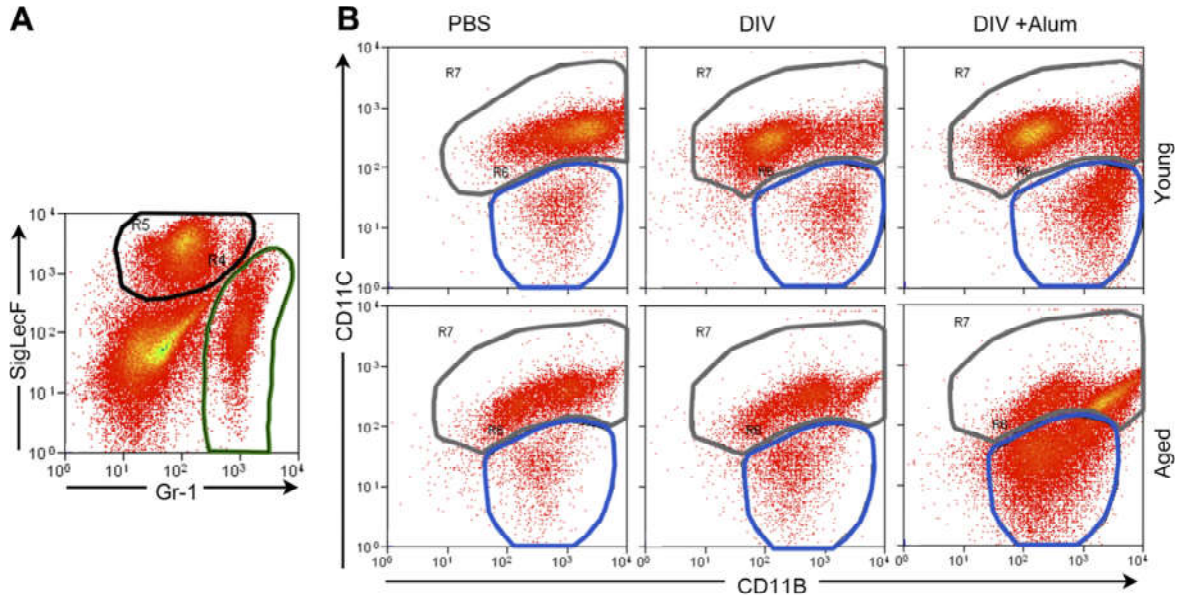


FIG. 8. Flow cytometry gating strategy for cell populations. (A) Representative (PBS-vaccinated) plot of $LCA^+$ lung cell populations. Neutrophils were defined as live cells, $LCA^+$, $Siglec^-$, and $GR\text{-}1^+$ (green gate). $SiglecF^+$ populations (black gate) from young and old mice were further analyzed, as shown in panel B. (B) Representative images of eosinophil ($CD11b^+$ and $CD11c^-$; blue gate) and alveolar macrophage ($CD11c^+$; gray gate) gates for young and aged mice vaccinated with PBS, DIV, or DIV plus alum.

*hoc* analysis showed the differences were enhanced by the alum adjuvant ($P = 0.04402$) (Fig. 9D). Vaccination with DIV clearly induces a strong eosinophilic infiltrate, independent of age and regardless of whether it protects from morbidity, and raises the possibility that DIV elicits immune pathology in the face of heterologous SARS challenge.

**Vaccine-induced eosinophilia is a common feature of N proteins across group 2b coronaviruses.** The data from our studies collectively demonstrated that eosinophilic infiltration occurs during DIV vaccination in both young and aged mouse populations, irrespective of the adjuvant and the challenge virus used. Previous data from our laboratory have shown that vaccination with VRPs expressing SARS N protein (VRP N) induces a similar eosinophilic phenotype while completely failing to protect against SARS CoV replication (11), suggesting that the eosinophilia may be driven by SARS N protein. To determine whether sequences intrinsic to SARS N protein or an N protein from a group 2b coronavirus closely related to SARS contribute to the induction of eosinophilia, we immunized mice with VRPs expressing SARS N, the N gene from BtCoV.279 (VRP 279 N), or an irrelevant antigen, VRP HA (containing the hemagglutinin gene from the PR8 strain of influenza virus). The BtCoV.279 N gene shares 95% sequence homology with the SARS N gene, with conservation across all the major domains of the N protein. Groups of mice immunized with $10^5$ IU of VRP N and VRP 279 N showed high antibody titers post boost (data not shown) and were challenged with $10^5$ PFU of rMA15 GDO3-S. This virus causes 15% weight loss in infected young BALB/c mice by day 4 postinfection (48). Mice from all the groups showed 15% weight loss by day 4 postinfection, with virus titers ranging up to $10^5$ PFU (data not shown), indicating failure of N gene-based vaccines to protect from virus replication. Histological analysis of Congo red-stained lung sections showed increased numbers of eosinophils proximal to airways in VRP N-immunized mice compared to VRP HA-immunized mice (Fig. 10A). Interestingly, enhanced influx of eosinophils was also found in regions proximal to the airways in lungs from mice immunized with VRP 279 N (Fig. 10A). Blind scoring of lung sections indicated a median count of 25 eosinophils per region in VRP N- and 279 N-immunized groups, whereas the VRP HA group showed a median count of 3 per region (Fig. 10B). These data clearly indicated that eosinophilia is driven by immune responses to sequences intrinsic to the SARS nucleocapsid protein and is conserved in N proteins across group 2b coronaviruses.

## DISCUSSION

The human coronaviruses HCoV 229E, HCoV OC43, and SARS-CoV, each likely originating from animal reservoirs, have demonstrated a high proclivity for coronaviruses to cross the species barrier, adapt, and colonize the human host. Though not currently circulating in humans, SARS-CoV, like other zoonotic viruses, remains a significant reemerging disease threat given its maintenance in animal reservoirs. The development of vaccines or therapeutics for SARS-CoV is complicated by several challenges: the presence of a large heterogeneous zoonotic reservoir of related strains, the resistance of highly susceptible aged populations to vaccination, and potential disease-enhancing complications of the vaccine formulations (11, 48, 61). Though many experimental SARS vaccine formulations have been developed, whole inactivated virus vaccines have the advantage of large-scale production, presentation of multiple epitopes, and conformation stability (2, 11, 13, 28, 33, 48, 60).

Aged populations are classically difficult to vaccinate and suffer increased disease pathologies following infection with a

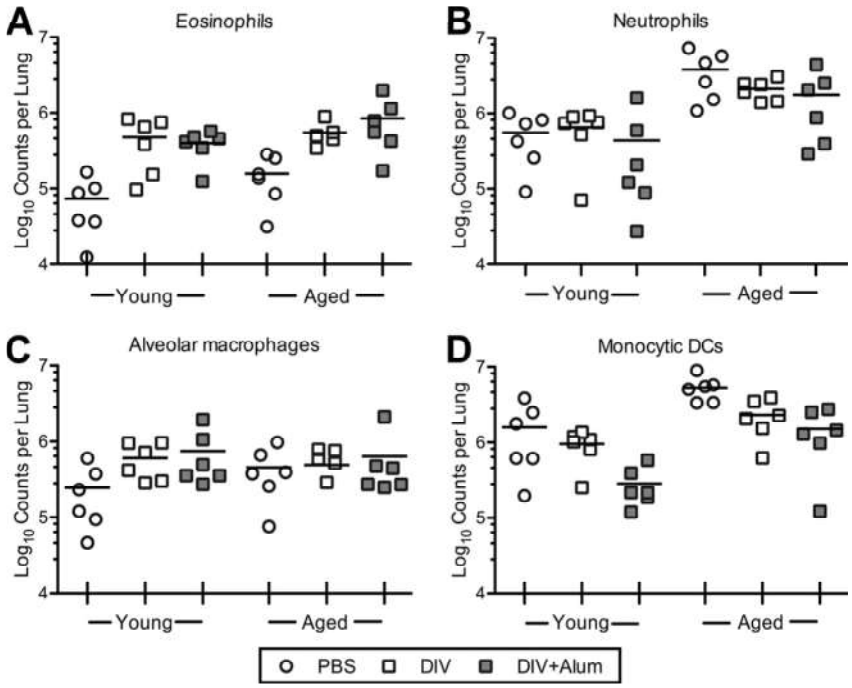


FIG. 9. Flow cytometric analysis of additional lung immune cell populations in young and aged mice following immunization and subsequent lethal challenge. Mice challenged with icHC/SZ/61/03-S were sacrificed 4 days postinfection, and the lungs were stained with an eight-color panel. Each point represents the cell population for an individual mouse. (A) Eosinophil counts for each of the vaccination groups ($n = 6$ per group). Regardless of the age of the mice, the eosinophil counts were significantly increased in both DIV- and DIV-plus-alum-immunized groups compared to mock-vaccinated groups ($F_{2,30} = 15.81$; $P < 1 \times 10^{-4}$). (B) For neutrophil counts, only age was a significant factor ($F_{1,30} = 24.7150$; $P = 2.525e{-}5$). (C) Alveolar macrophage counts were significantly affected by immunogens in young, but not aged, animals, with *post hoc* analysis indicating that both DIV and DIV-plus-alum groups significantly differed from mock-vaccinated groups ($F_{2,30} = 3.5534$; $P = 0.04121$). (D) mDCs were also significantly affected by age ($F_{1,30} = 20.3622$; $P = 9.193e{-}05$), as well as immunogen ($F_{2,30} = 9.5681$; $P = 0.0006107$), with *post hoc* analysis indicating significant reductions in mDC counts in DIV-plus-alum groups relative to both DIV and mock-vaccinated groups.

variety of respiratory viruses, including influenza virus, RSV, HCoV OC43, and SARS-CoV (14). Until recently, most published assessments of SARS-CoV vaccine efficacy utilized models capable of assessing only viral replication or antibody induction, and they are routinely conducted in animal models that neglect important human disease presentations (11, 17, 33, 40, 46, 50). While necessary, these assessments are incomplete, especially because more robust lethal-challenge models have been developed that recapitulate severe end stage lung disease pathologies and allow assessment of the potential complications of senescence (42, 43, 45, 48, 59). As shown here, a vaccine that appears protective in young animals is much less protective, and potentially pathogenic, in an aged-animal model.

SARS-CoV emerged from a heterologous pool of closely related animal strains, suggesting that future outbreak emergences will likely involve strains with unique changes in the S glycoprotein. The viral strains used in this study represent a homologous lethal challenge virus (icMA15), as well as a nonlethal human heterologous virus (icGD03-S) and a lethal zoonotic virus (icHC/SZ/61/03-S), which allowed us to directly test whether DIV was capable of providing effective protection against heterologous viruses in both young and highly susceptible aged populations. Importantly, the DIV vaccine provided partial protection against both homologous and heterologous challenge in young animals, and this protective effect was enhanced by alum adjuvant. In contrast, even the adjuvanted DIV vaccine failed to protect against virus-induced disease and viral replication following homologous or heterologous challenge in aged animals. Perhaps most importantly, though DIV plus alum protected against viral replication, disease, and respiratory pathology following homologous viral challenge (icMA15) in young animals, which is consistent with prior reports (17, 46, 50), both DIV alone and DIV plus alum failed to protect against respiratory pathology following homologous challenge in aged animals, and both vaccine formulations failed to protect against respiratory pathology following heterologous challenge in mice of any age (Fig. 4 and 5). These results further demonstrate the difficulty in eliciting protective immune responses in highly susceptible elderly population and indicate that in the face of a reemergent SARS virus, likely antigenically heterologous from the 2002 outbreak strain, existing vaccine formulations are unlikely to provide protective immunity.

In addition to the general failure of the DIV or DIV-plus-alum vaccines to elicit protective immunity against heterologous SARS viruses or to provide protection even against homologous viral challenge in aged animals, both the DIV and DIV-plus-alum vaccine formulations result in significantly enhanced immune pathology within the lungs compared to control animals. Although adjuvanted DIV protected young animals from morbidity and mortality following lethal challenges, the heterologous virus, icHC/SZ/61/03-S, induced a lung pathology that was more severe in vaccinated than in

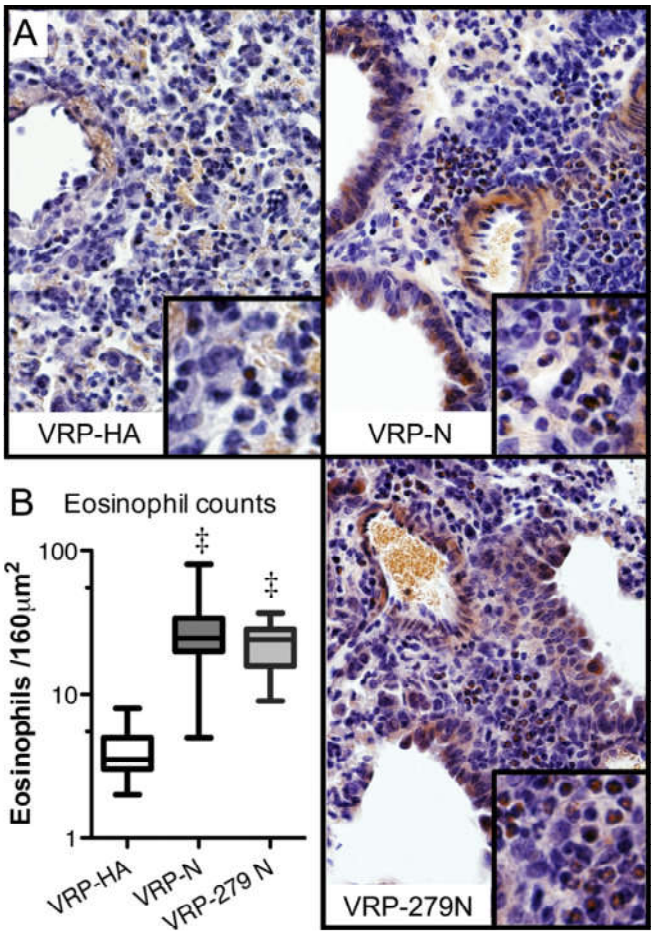


FIG. 10. Eosinophilia influx is conserved across group 2b N proteins. Young mice immunized with VRPs expressing the SARS N protein (VRP N); the N protein from another group 2b bat coronavirus, BtCoV.279 (VRP 279 N); or an irrelevant antigen (VRP-HA) were challenged with icGD03, and the lungs were taken 4 days postinfection. (A) Representative images of lung sections (×400) stained with Congo red. The inset shows areas of dense inflammatory infiltrate at higher magnification. (B) Both the SARS N and BtCoV.279 N proteins induce a significant eosinophilic inflammatory influx compared to the irrelevant antigen. ‡, $P < 0.0001$.

unvaccinated mice (Fig. 4). This increased pathology was not correlated with weight loss or mortality through day 4 postinfection (Fig. 3), but the increased immune infiltrate indicates the vaccine is not fully protective against heterologous challenges. Further, in aged animals recalcitrant to immunization, insufficient protective immunity correlated with significantly increased immunopathology. Thus, evidence of enhanced disease subsequent to vaccination was evident in both heterologous challenge models and models of immune senescence.

In each of the experiments conducted here, immunization with the whole inactivated SARS vaccine induced increased inflammatory infiltrates and pulmonary eosinophilia upon subsequent challenge, demonstrating the potential for dangerous clinical complications. This is consistent with two prior studies of vaccine formulations incorporating SARS N, where N-specific immune responses resulted in enhanced eosinophilic immune pathology (11, 61). This pathological signature is reminiscent of the two known human examples of vaccine-induced immunopathology, atypical measles and enhanced RSV. For both of these vaccine-induced immunopathologies, infection subsequent to vaccination resulted in failure to control viral replication, enhanced clinical disease, and a pathology characterized by increased complement deposition and inflammation, skewing toward Th2 responses, and eosinophilic influx (38). The cytokine profiles of DIV-plus-alum-vaccinated and icHC/SZ/61/03-challenged mice showed increased levels of Th2 effector cytokines and eosinophil chemokines (IL-5, IL-13, and CCL11/eotaxin) compared to mock-vaccinated groups (Fig. 8). In contrast, IFN-γ and IL-4 (Th1- and Th2-inducing cytokines) were unchanged at 2 and 4 days postinfection, likely because the peak mRNA levels for these inducing cytokines were earlier in the time course of infection.

As previous studies had indicated peak eosinophilia at 4 days postinfection, we assessed lung eosinophilia by both histopathology and flow cytometry at this time point, quantifying significant increases in the lungs of vaccinated mice following CoV challenge (11). Eosinophilia was present independent of age and independent of the alum adjuvant, although adjuvant did increase the magnitude of the eosinophilic influx. DIV-induced eosinophilic influx was present even in the animals that were protected from morbidity and mortality. When this protection was absent, eosinophilic immunopathology was a dominant response more severe than the viral pathology seen in unvaccinated controls. The eosinophilia in clinically protected animals may thus serve as a marker for potentially pathogenic immune responses. While recent studies have argued that eosinophils are not the primary mediators of RSV vaccine-induced immune pathology, they may contribute to increased airway hyperresponsive conditions, including asthma, and the pathophysiology of viral infections (6, 20).

Only eosinophils were consistently and significantly increased in response to vaccination with DIV. In contrast, neutrophils and monocytic DC populations were significantly affected by age, and monocytic DCs were decreased as a function of vaccination. The greater population of neutrophils in aged animals following challenge, independent of vaccination, suggests that neutrophils may contribute to the increased severity of SARS-CoV pathogenesis in the aged. A pathogenic role for neutrophils in infection has been demonstrated for other respiratory viruses, including influenza virus, suggesting conserved mechanisms of enhanced respiratory pathology in the aged (26, 32).

SARS-CoV-targeted neutralizing antibodies are sufficient to provide complete immunity against lethal SARS challenges in multiple animal models and show evidence of controlling disease severity in human infections (4, 5, 11, 15, 44, 64, 67). Spike-specific antibodies are both neutralizing and protective up to 1 year postvaccination in mice, while anti-nucleocapsid antibodies are neither neutralizing nor protective and, further, appear to be detrimental to the longevity of protective antibodies (11, 61). This deleterious effect does not appear to be an antibody-dependent enhancement (ADE), since passive transfer was unable to replicate the immunopathology, though low posttransfer antibody titers preclude definitive exclusion of this potential mechanism (11, 58).

While multiple major and minor SARS-CoV antigens are incorporated in DIV, the N protein is the most likely agent of

eosinophilic immunopathology (34). N is a strongly immunogenic protein (7, 9, 37, 65), is the most abundant protein in infection (34), and has been shown in prior studies to induce immunopathology when delivered in isolation (66). This nucleocapsid-induced enhancement is not apparent in animals with appreciable levels of neutralizing antibodies, indicating that the induction of sufficiently neutralizing antibody responses can protect against SARS vaccine-induced immune pathology. However, the results presented here clearly demonstrate that in situations where individuals fail to mount protective anti-SARS responses, as is the case with heterologous viral challenge or in immune senescence, the DIV-vaccinated individuals are at significant risk for vaccine-induced immune pathology. With this in mind, it will also be important to determine the mechanisms by which N vaccination promotes immune pathology, with a key question being whether pathology is simply due to a nonprotective response against N or if N vaccination actively skews the host immune response to promote immune pathology. Given that N has been shown to modulate innate immunity and to act as an interferon antagonist, it is possible that N sufficiently alters the host immune response to induce a Th2 skew and subsequent inflammatory pathology (21). Indeed, immunization with N appears to induce a Th2 skewing of the immune response regardless of the adjuvant or formulation, suggesting the nucleocapsid protein alone may well be the defining factor in CoV vaccine-induced enhancement (11, 61; K. Long, D. Deming, R. Baric, and M. Heise, unpublished data). Therefore, additional studies are required to assess whether N′s innate immunomodulatory activity is linked to the N vaccine-induced immune pathology, and if so, whether this reflects a more general trait of viral interferon antagonists in modulating the downstream host adaptive immune response.

The major conclusion that can be drawn from these studies is that although DIV SARS vaccines do elicit protection under optimal conditions (homologous challenge in immunocompetent individuals), more stringent challenges reveal likely failures. If DIV vaccine approaches are to be used for SARS in the future, efforts must be made to improve the quality and magnitude of the vaccine-induced immune response while limiting the vaccine's capacity to induce immune pathology. The whole-virus vaccine used in this study was doubly inactivated by UV irradiation and formalin (50). Formalin-inactivated vaccines are suggested to skew the immune response toward a Th2 response, producing higher levels of IL-4 and increasing the relative contribution of IgG2a isotypes (31, 57). Previously, formalin inactivation leading to a disruption of fusion glycoproteins or addition of carbonyl groups had been blamed for the skewing of formalin-inactivated RSV (FI-RSV) immune responses (31, 38). However, recent studies suggest that inactivation by alternate methods still results in a Th2 skew and immunopathology and that it is a failure of affinity maturation that results in nonprotective responses and subsequent antibody-mediated enhancement (10, 57). Furthermore, the fact that the DIV vaccine did elicit neutralizing antibody responses and protection against homologous challenge in young animals suggests that the DIV-induced pathology did not simply represent a loss of antigenic epitopes. Therefore, we do not think the method of inactivation is necessarily responsible for immunopathology associated with DIV, but rather, that any SARS vaccines that include the nucleocapsid protein should be investigated for challenge-induced enhancement.

The results presented here reinforce the need to find methods to enhance the protective S-specific immune response while minimizing potentially pathological anti-N response. Our observation that immunization with BtCoV.279 N, which has high sequence similarity to SARS N, also induces eosinophila indicates that sequences intrinsic to N protein that are conserved across group 2b coronaviruses may drive this immune-mediated pathology. The amino acids responsible for this response need to be mapped. Assessment of N-induced immune pathology by sequentially divergent CoV N proteins may allow the design of chimeric SARS CoVs that could serve as vaccines devoid of immune pathology. In both young and aged mice, adjuvanting with alum increases the immunogenicity of the DIV, concordant with many earlier studies using this adjuvant (50). In young mice, approximately one-half of the animals mounted neutralizing antibodies following DIV vaccination, and all achieved neutralizing titers when DIV was adjuvanted with alum (Fig. 2). However, only half the aged mice were capable of mounting neutralizing antibody titers to DIV plus alum, and none mounted such responses without the adjuvant. Alum is one of the few adjuvants approved for use in human vaccine formulations and functions to stimulate Th2 immunity, a potentially confounding factor in the induction of immunopathology. We briefly assessed an alternative adjuvant, VAP, which is reported to stimulate Th1 immunity (18, 53, 56, 57). In contrast to reports of success in young mice, the VAP-adjuvanted formulation in aged mice ablated rather than enhanced the protective response to DIV; subsequently challenged mice showed morbidity and mortality rates comparable to those in unvaccinated controls (data not shown) (55, 56). While the mechanism of this ablation has not been defined, the VAP adjuvant likely functions through cross-presentation of exogenous antigens within antigen-presenting cells, a process impaired in age-associated immunosenescence (16). VEE formulations incorporating the wild-type 3000 glycoprotein show better immunogenicity in aged animals, likely due to improved cross-presentation over the attenuated 3014 glycoprotein, suggesting that alternative VAP formulations may be more effective (48). Therefore, if DIV approaches are to be considered for SARS or other respiratory coronaviruses, we feel that it will be important to rigorously test the vaccine and potential adjuvant in the aged-mouse model to assess both efficacy and potential immune pathology in the face of immune senescence and/or heterologous viral challenges.

Emergent zoonotic viruses present novel and shifting targets for vaccine design. The clear deficiency of the double-inactivated SARS vaccine against challenge models with divergent spike glycoproteins highlights the need for vaccines that induce broadly neutralizing immune responses. Further, impartial conservation of viral antigens cannot be considered a benefit to vaccine formulations for coronaviruses when select immunogens induce detrimental immune responses upon challenge. The N-induced pathogenic responses appear to be masked by S-targeted neutralizing antibodies but become dominant once the protective immunity wanes. In the case of SARS-like CoV, we cannot expect zoonotic variation to reduce specificity for N more readily than for S, as the S glycoproteins of multiple isolates show greater sequence variation and readily evolve

over the course of an epidemic (19, 22, 44). Further, the conservation of N across group 2b coronaviruses and the demonstrated conservation of N-induced immunopathology raise the possibility that challenge with nonepidemic coronavirus strains may induce eosinophilic immunopathology in vaccinated populations. Despite the difficulty of vaccine design for zoonotic viruses such as coronaviruses, paramyxoviruses, and filoviruses, a growing pool of sequence data for zoonotic isolates; the rapidity of sequencing and isolation in the case of outbreaks; synthetic-gene design; and the multiple vectored, inactivation, or antibody-generating platform technologies available ensure that vaccines can be readily formulated in case of novel outbreaks (1). The challenge for researchers and clinicians is to validate these vaccines in strong animal models and to confirm and enhance vaccine efficacy in aged individuals. Identifying the vaccine components that induce protective immunity in aging individuals will be essential to protecting this vulnerable population. The data presented here indicate that SARS-CoV, coupled with a panel of heterologous zoonotic precursor viruses, represents a tractable model system to evaluate the molecular mechanisms governing immunosenescence and its impact on emerging virus pathogenesis and vaccine efficacy.

## ACKNOWLEDGMENTS

This work was supported by grants from the National Institutes of Health, Division of Allergy and Infectious Diseases (AI075297, U54AI080680, and U54AI081680-01), and the UNC-CH Medical Science Training Program (T32GM008719 [M.B.]).

We thank Kanta Subbarao at the NIH for generously providing the icMA15 virus. We recognize the generous gift of the adjuvanted and unadjuvanted DIV from BEI. We also thank Vineet Menachery for help in manuscript preparation.

## REFERENCES

1. **Becker, M. M., et al.** 2008. Synthetic recombinant bat SARS-like coronavirus is infectious in cultured cells and in mice. Proc. Natl. Acad. Sci. U. S. A. **105:**19944–19949.
2. **Bisht, H., et al.** 2004. Severe acute respiratory syndrome coronavirus spike protein expressed by attenuated vaccinia virus protectively immunizes mice. Proc. Natl. Acad. Sci. U. S. A. **101:**6641–6646.
3. **Booth, C., et al.** 2003. Clinical features and short-term outcomes of 144 patients with SARS in the greater Toronto area. JAMA **289:**2801–2809.
4. **Bossart, K. N., et al.** 2009. A neutralizing human monoclonal antibody protects against lethal disease in a new ferret model of acute nipah virus infection. PLoS Pathog. **5:**e1000642.
5. **Cameron, M., et al.** 2007. Interferon-mediated immunopathological events are associated with atypical innate and adaptive immune responses in severe acute respiratory syndrome (SARS) patients. J. Virol. **81:**8692–8706.
6. **Castilow, E. M., K. L. Legge, and S. M. Varga.** 2008. Cutting edge: eosinophils do not contribute to respiratory syncytial virus vaccine-enhanced disease. J. Immunol. **181:**6692–6696.
7. **Chen, Z., et al.** 2004. Antigenicity analysis of different regions of the severe acute respiratory syndrome coronavirus nucleocapsid protein. Clin. Chem. **50:**988–995.
8. **Chinese SARS Molecular Epidemiology Consortium.** 2004. Molecular evolution of the SARS coronavirus during the course of the SARS epidemic in China. Science **303:**1666–1669.
9. **Chow, S. C. S., et al.** 2006. Specific epitopes of the structural and hypothetical proteins elicit variable humoral responses in SARS patients. J. Clin. Pathol. **59:**468–476.
10. **Delgado, M. F., et al.** 2009. Lack of antibody affinity maturation due to poor Toll-like receptor stimulation leads to enhanced respiratory syncytial virus disease. Nat. Med. **15:**34–41.
11. **Deming, D., et al.** 2006. Vaccine efficacy in senescent mice challenged with recombinant SARS-CoV bearing epidemic and zoonotic spike variants. PLoS Med. **3:**e525.
12. **Donnelly, C. A., et al.** 2003. Epidemiological determinants of spread of causal agent of severe acute respiratory syndrome in Hong Kong. Lancet **361:**1761–1766.
13. **Enjuanes, L., et al.** 2008. Vaccines to prevent severe acute respiratory syndrome coronavirus-induced disease. Virus Res. **133:**45–62.
14. **Goodwin, K., C. Viboud, and L. Simonsen.** 2006. Antibody response to influenza vaccination in the elderly: a quantitative review. Vaccine **24:**1159–1169.
15. **Greenough, T. C., et al.** 2005. Development and characterization of a severe acute respiratory syndrome-associated coronavirus-neutralizing human monoclonal antibody that provides effective immunoprophylaxis in mice. J. Infect. Dis. **191:**507–514.
16. **Gruver, A. L., L. L. Hudson, and G. D. Sempowski.** 2007. Immunosenescence of ageing. J. Pathol. **211:**144–156.
17. **He, Y., Y. Zhou, P. Siddiqui, and S. Jiang.** 2004. Inactivated SARS-CoV vaccine elicits high titers of spike protein-specific antibodies that block receptor binding and virus entry. Biochem. Biophys. Res. Commun. **325:**445–452.
18. **HogenEsch, H.** 2002. Mechanisms of stimulation of the immune response by aluminum adjuvants. Vaccine **20:**S34–S39.
19. **Hou, Y.-X., et al.** 2010. Immunogenicity of the spike glycoprotein of Bat SARS-like coronavirus. Virol. Sin. **25:**36–44.
20. **Ishioka, T., et al.** 2011. Effects of respiratory syncytial virus infection and major basic protein derived from eosinophils in pulmonary alveolar epithelial cells (A549). Cell Biol. Int. **35:**467–474.
21. **Kopecky-Bromberg, S. A., L. Martínez-Sobrido, M. Frieman, R. A. Baric, and P. Palese.** 2007. Severe acute respiratory syndrome coronavirus open reading frame (ORF) 3b, ORF 6, and nucleocapsid proteins function as interferon antagonists. J. Virol. **81:**548–557.
22. **Lau, S. K. P., et al.** 2005. Severe acute respiratory syndrome coronavirus-like virus in Chinese horseshoe bats. Proc. Natl. Acad. Sci. U. S. A. **102:**14040–14045.
23. **Li, W., et al.** 2005. Bats are natural reservoirs of SARS-like coronaviruses. Science **310:**676–679.
24. **Lin, J.-T., et al.** 2007. Safety and immunogenicity from a phase I trial of inactivated severe acute respiratory syndrome coronavirus vaccine. Antivir. Ther. **12:**1107–1113.
25. **LoBue, A. D., J. M. Thompson, L. Lindesmith, R. E. Johnston, and R. S. Baric.** 2009. Alphavirus-adjuvanted norovirus-like particle vaccines: heterologous, humoral, and mucosal immune responses protect against murine norovirus challenge. J. Virol. **83:**3212–3227.
26. **Malcolm, K. C., et al.** 2011. Bacteria-specific neutrophil dysfunction associated with interferon-stimulated gene expression in the acute respiratory distress syndrome. PLoS One **6:**e21958.
27. **Marshall, E., and M. Enserink.** 2004. Medicine. Caution urged on SARS vaccines. Science **303:**944–946.
28. **Martin, J. E., et al.** 2008. A SARS DNA vaccine induces neutralizing antibody and cellular immune responses in healthy adults in a phase I clinical trial. Vaccine **26:**6338–6343.
29. **McElhaney, J. E., J. W. Hooton, N. Hooton, and R. C. Bleackley.** 2005. Comparison of single versus booster dose of influenza vaccination on humoral and cellular immune responses in older adults. Vaccine **23:**3294–3300.
30. **Meyerholz, D. K., M. A. Griffin, E. M. Castilow, and S. M. Varga.** 2009. Comparison of histochemical methods for murine eosinophil detection in an RSV vaccine-enhanced inflammation model. Toxicol. Pathol. **37:**249–255.
31. **Moghaddam, A., et al.** 2006. A potential molecular mechanism for hypersensitivity caused by formalin-inactivated vaccines. Nat. Med. **12:**905–907.
32. **Narasaraju, T., et al.** 2011. Excessive neutrophils and neutrophil extracellular traps contribute to acute lung injury of influenza pneumonitis. Am. J. Pathol. **179:**199–210.
33. **Netland, J., et al.** 2010. Immunization with an attenuated severe acute respiratory syndrome coronavirus deleted in E protein protects against lethal respiratory disease. Virology **399:**120–128.
34. **Neuman, B. W., et al.** 2006. Supramolecular architecture of severe acute respiratory syndrome coronavirus revealed by electron cryomicroscopy. J. Virol. **80:**7918–7928.
35. **Normile, D.** 2005. Virology researchers tie deadly SARS virus to bats. Science **309:**2154–2155.
36. **Peiris, J. S. M., et al.** 2003. Clinical progression and viral load in a community outbreak of coronavirus-associated SARS pneumonia: a prospective study. Lancet **361:**1767–1772.
37. **Peng, H., L.-T. Yang, L.-Y. Wang, J. Li, J. Huang, Z.-Q. Lu, R. A. Koup, R. T. Bailer, and C.-Y Wu.** 2006. Long-lived memory T lymphocyte responses against SARS coronavirus nucleocapsid protein in SARS-recovered patients. Virology **351:**466–475.
38. **Polack, F.** 2007. Atypical measles and enhanced respiratory syncytial virus disease (ERD) made simple. Pediatr. Res. **62:**111.
39. **Roberts, A., et al.** 2007. A mouse-adapted SARS-coronavirus causes disease and mortality in BALB/c mice. PLoS Pathog. **3:**e5.
40. **Roberts, A., et al.** 2010. Immunogenicity and protective efficacy in mice and hamsters of a β-propiolactone inactivated whole virus SARS-CoV vaccine. Viral Immunol. **23:**509–519.
41. **Roberts, A., et al.** 2008. Animal models and vaccines for SARS-CoV infection. Virus Res. **133:**20–32.
42. **Roberts, A., et al.** 2005. Aged BALB/c mice as a model for increased severity of severe acute respiratory syndrome in elderly humans. J. Virol. **79:**5833–5838.

43. **Rockx, B., et al.** 2009. Early upregulation of acute respiratory distress syndrome-associated cytokines promotes lethal disease in an aged-mouse model of severe acute respiratory syndrome coronavirus infection. J. Virol. **83:** 7062–7074.
44. **Rockx, B., et al.** 2008. Structural basis for potent cross-neutralizing human monoclonal antibody protection against lethal human and zoonotic severe acute respiratory syndrome coronavirus challenge. J. Virol. **82:**3220–3235.
45. **Rockx, B., et al.** 2007. Synthetic reconstruction of zoonotic and early human severe acute respiratory syndrome coronavirus isolates that produce fatal disease in aged mice. J. Virol. **81:**7410–7423.
46. **See, R. H., et al.** 2008. Severe acute respiratory syndrome vaccine efficacy in ferrets: whole killed virus and adenovirus-vectored vaccines. J. Gen. Virol. **89:**2136–2146.
47. **Sheahan, T., D. Deming, E. Donaldson, R. Pickles, and R. Baric.** 2006. Resurrection of an "extinct" SARS-CoV isolate GD03 from late 2003. Adv. Exp. Med. Biol. **581:**547–550.
48. **Sheahan, T., et al.** 2011. Successful vaccination strategies that protect aged mice from lethal influenza and lethal heterologous SARS-CoV challenge. J. Virol. **85:**217–230.
49. **Song, H., et al.** 2005. Cross-host evolution of severe acute respiratory syndrome coronavirus in palm civet and human. Proc. Natl. Acad. Sci. U. S. A. **102:**2430–2435.
50. **Spruth, M., et al.** 2006. A double-inactivated whole virus candidate SARS coronavirus vaccine stimulates neutralising and protective antibody responses. Vaccine **24:**652–661.
51. **Stockman, L. J., R. Bellamy, and P. Garner.** 2006. SARS: systematic review of treatment effects. PLoS Med. **3:**e343.
52. **Subbarao, K., et al.** 2004. Prior infection and passive transfer of neutralizing antibody prevent replication of severe acute respiratory syndrome coronavirus in the respiratory tract of mice. J. Virol. **78:**3572–3577.
53. **Takasuka, N., et al.** 2004. A subcutaneously injected UV-inactivated SARS coronavirus vaccine elicits systemic humoral immunity in mice. Int. Immunol. **16:**1423–1430.
54. **Thompson, J. M., et al.** 2006. Mucosal and systemic adjuvant activity of alphavirus replicon particles. Proc. Natl. Acad. Sci. U. S. A. **103:**3722–3727.
55. **Thompson, J. M., A. C. Whitmore, H. F. Staats, and R. Johnston.** 2008. The contribution of type I interferon signaling to immunity induced by alphavirus replicon vaccines. Vaccine **26:**4998–5003.
56. **Thompson, J. M., A. C. Whitmore, H. F. Staats, and R. E. Johnston.** 2008. Alphavirus replicon particles acting as adjuvants promote CD8+ T cell responses to co-delivered antigen. Vaccine **26:**4267–4275.
57. **Tsunetsugu-Yokota, Y., M. Ato, Y. Takahashi, S.-I. Hashimoto, T. Kaji, M. Kuraoka, K.-I. Yamamoto, Y.-Y. Mitsuki, T. Yamamoto, M. Oshima, K. Ohnishi, and T. Takemori.** 2007. Formalin-treated UV-inactivated SARS coronavirus vaccine retains its immunogenicity and promotes Th2-type immune responses. Jpn. J. Infect. Dis. **60:**106–112.
58. **Ubol, S., and S. B. Halstead.** 2010. How innate immune mechanisms contribute to antibody-enhanced viral infections. Clin. Vaccine Immunol. **17:** 1829–1835.
59. **Vogel, L. N., et al.** 2007. Utility of the aged BALB/c mouse model to demonstrate prevention and control strategies for severe acute respiratory syndrome coronavirus (SARS-CoV). Vaccine **25:**2173–2179.
60. **Yang, Z.-Y., et al.** 2004. A DNA vaccine induces SARS coronavirus neutralization and protective immunity in mice. Nature **428:**561–564.
61. **Yasui, F., et al.** 2008. Prior immunization with severe acute respiratory syndrome (SARS)-associated coronavirus (SARS-CoV) nucleocapsid protein causes severe pneumonia in mice infected with SARS-CoV. J. Immunol. **181:**6337–6348.
62. **Yip, C. W., et al.** 2009. Phylogenetic perspectives on the epidemiology and origins of SARS and SARS-like coronaviruses. Infect. Genet. Evol. **9:**1185–1196.
63. **Yount, B., et al.** 2003. Reverse genetics with a full-length infectious cDNA of severe acute respiratory syndrome coronavirus. Proc. Natl. Acad. Sci. U. S. A. **100:**12995–13000.
64. **Zhang, J.-S., et al.** 2005. A serological survey on neutralizing antibody titer of SARS convalescent sera. J. Med. Virol. **77:**147–150.
65. **Zhong, X., et al.** 2005. B-cell responses in patients who have recovered from severe acute respiratory syndrome target a dominant site in the S2 domain of the surface spike glycoprotein. J. Virol. **79:**3401–3408.
66. **Zhu, Y. G., and J. M. Qu.** 2009. Differential characteristics of the early stage of lung inflammation induced by SARS-CoV nucleocapsid protein related to age in the mouse. Inflamm. Res. **58:**312–320.
67. **Zhu, Z., et al.** 2007. Potent cross-reactive neutralization of SARS coronavirus isolates by human monoclonal antibodies. Proc. Natl. Acad. Sci. U. S. A. **104:**12123–12128.